Interrupted Helical Structure of Grafted Polypeptides in Brush-Like Macromolecules

Jing Wang,[†] Hua Lu,[‡] Yuan Ren,[§] Yanfeng Zhang,[‡] Martha Morton,[§] Jianjun Cheng,[*,‡] and Yao Lin[*,†,§]

[†]Polymer Program, Institute of Materials Science, University of Connecticut, Storrs, Connecticut 06269, United States

[‡]Department of Materials Science and Engineering, University of Illinois at Urbana—Champaign, Urbana, Illinois 61801, United States

[§]Department of Chemistry, University of Connecticut, Storrs, Connecticut 06269, United States

Ⓢ Supporting Information

ABSTRACT: Brush-like polymers are a type of graft polymers with densely and regularly spaced side chains. Their unique topologies and large sizes afforded a number of potential applications in nanotechnology. Incorporating helical polypeptides as grafted chains in brush polymers may allow for the construction of large macromolecules with structurally well-defined, rod-like domains. However, due to a congested local environment in brush polymers, the conformational structure of grafted polypeptides can deviate from the "rigid-rod" α-helical structure observed in homopolypeptides. Because of synthetic challenges, the effect of macromolecular environments on the conformational structures of grafted polypeptides has not been systematically studied in brush polymers. Here we synthesized a small library of polynorbornene-g-poly(γ-benzyl-L-glutamate) (PN-g-PBLG) with variable PN, PBLG lengths and grafting densities, and we studied solvent induced helix—coil transition of grafted PBLGs in these brush polymers to explore their specific conformational structures. Instead of forming rigid-rod α-helices in helicogenic solvents, the grafted PBLGs in PN-g-PBLG, especially those with high grafting density and high molecular weights (MWs), adopt interrupted helical structures that can be represented by a "broken rod" model, which was also confirmed by the nuclear overhauser enhancement spectroscopy (NOESY) experiments. The behavior also exists in other types of grafted polypeptides in brush polymers, e.g., PN-g-poly(ε-benzyloxycarbonyl-L-lysine) (PN-g-PZLL). These findings and the structural analysis methods we developed in this study provide the guidance to the rational design and characterization of polypeptide-containing macromolecules with complex architectures.
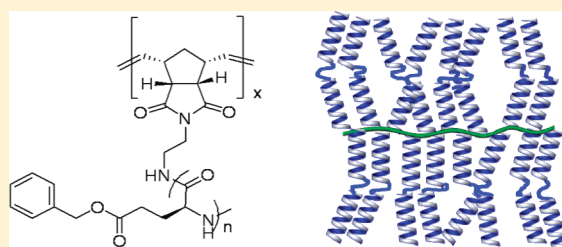
■ INTRODUCTION

The development of controlled ring-opening polymerization (ROP) of amino acid N-carboxyanhydrides (NCAs) allows for the synthesis of polypeptides with controlled molecular weights (MWs) and narrow molecular weight distributions (MWDs).[1−12] Unlike many other synthetic polymers that form flexible, coil-like structures, synthetic polypeptides can adopt rigid rod-like, α-helical structures with large persistence lengths (Figure 1A).[13−16] These predetermined secondary structural components, when incorporated into different macromolecular architectures (e.g., block copolymers, multiarms or brush-like polymers), may allow for the construction of large and complex, yet structurally well-defined, macromolecules.[17−24] Polypeptide-containing brush polymers are particularly interesting as their conformations, assembly behaviors and physical properties are largely controlled by the backbone architecture and the interactions among the grafted polymeric chains.[18,21,25−27] New applications are expected to arise from the unique, highly dense macromolecular architectures and the controllable chain interactions from the grafted polypeptides in these brush polymers.

Contrary to common belief, α-helical polypeptides cannot always be regarded as ideal rigid rods, and in many situations, they are better represented by a "broken rod" model (Figure 1B) when the intrachain hydrogen bonds that stabilizes the α-helices are disrupted.[13] Such interrupted helical structure has been reported for poly(γ-benzyl-L-glutamate) (PBLG) in highly concentrated solutions or under confinement of nanodomains in bulk, as the helical structures are disrupted by the extensive intermolecular interactions.[13−15] Extended from these findings, we postulate that when helical polypeptide chains are in close proximity to each other in brush polymers, the extensive interchain interactions in the grafted polypeptides will also lead to formation of "broken rod" structures (Figure 1C). These potential structural changes in grafted polypeptides demand in-depth examination, as the grafted chains govern the overall structures, physical properties and assembly behaviors of the brush polymers. However, the effect of macromolecular environments on the structure of grafted polypeptides has not been systematically studied in brush polymers, due to challenges in the synthesis of these macromolecules and the difficulties in distinguishing
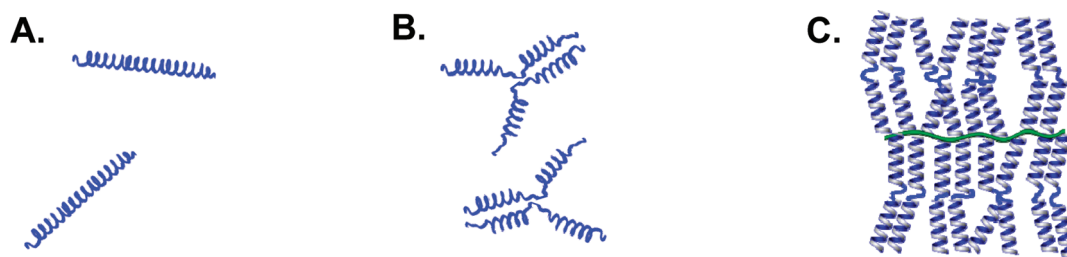
Figure 1. Schematic illustration of (A) helical polypeptide chains with ideal rigid-rod like structure (e.g., in helicogenic solvent), (B) helical polypeptide chains that adopt a "broken rod" like structure (e.g., in a highly concentrated solution, or under a locally confined environment in bulk), and (C) a densely grafted brush-like macromolecule bearing polypeptide chains with "broken rod" structures arising from extensive interactions among the grafted chains.

the subtle structural variations of polypeptide chains in complex macromolecules.

Recently, we reported that polypeptide-grafted brush polymers can be readily synthesized via integrated ring-opening metathesis of polymerization (ROMP) and polymerization of amino acid N-caroxyanhydrides (NCA).[7] Given that numerous ROMP and NCA monomers are available, this one-pot polymerization technique allows easy access to numerous polypeptide-containing brush polymers with controlled compositions and structures. In this study, we apply this new polymerization method to synthesize a small library of brush-like polynorbornene-g-poly(γ-benzyl-L-glutamate) (PN-g-PBLG) polymers with controlled PN and PBLG lengths and PBLG grafting densities. Solvent induced helix−coil transitions of polypeptides and nuclear overhauser enhancement spectroscopy (NOESY) experiments were then carried out to investigate the conformational structures of the grafted PBLGs in these brush polymers in solution. By establishing a reference system using well studied homo PBLG and a control system using diblock PBLG, we were able to determine the structure of the grafted PBLGs in response to different PBLG chain lengths and grafting densities, and confirmed the formation of the "broken-rod" structure of grafted PBLGs in these brush polymers. Similar interrupted helical structures were also found in other types of grafted polypeptides in brush polymers, e.g. PN-g-poly(ε-benzyloxycarbonyl-L-lysine) (PN-g-PZLL).

■ EXPERIMENTAL SECTION

General Data. All chemicals were purchased from Sigma-Aldrich (St. Louis, MO) and used as received unless otherwise specified. Anhydrous dimethylformamide (DMF) was dried by a column packed with 4 Å molecular sieves and stored in a glovebox. Tetrahydrofuran (THF) and hexane were dried by a column packed with alumina and stored in a glovebox. Anhydrous triethylamine (TEA) was prepared by treating commercial TEA (Sigma, St. Louis, MO) with KOH for 2 days, followed by distillation under nitrogen. Grubbs catalyst,[6,28] N-(N′-trimethylsilylaminoethyl)-5-norbornene-endo-2,3-dicarboximide,[12] N-benzyl-5-norbornene-endo-2,3-dicarboximide and Glu-NCA were prepared by following previously reported procedures.[29]

Characterization. NMR spectra were recorded on a Varian UI400 MHz, a UI500NB MHz, a VXR-500 MHz or a Bruker DRX 500 MHz spectrometer for polymer characterization. Tandem gel permeation chromatography (GPC) experiments were performed on a system equipped with an isocratic pump (Model 1100, Agilent Technology, Santa Clara, CA), a DAWN HELEOS 18-angle laser light scattering detector (also known as multiangle laser light scattering (MALLS) detector, Wyatt Technology, Santa Barbara, CA) and an Optilab rEX

refractive index detector (Wyatt Technology, Santa Barbara, CA). The detection wavelength of HELEOS was set at 658 nm. Separations were performed using serially connected size exclusion columns (100 Å, 500 Å, 10^3 Å and 10^4 Å Phenogel columns, 5 μm, 300 × 7.8 mm, Phenomenex, Torrance, CA) at 60 °C using DMF containing 0.1 M LiBr as the mobile phase. The MALLS detector is calibrated using pure toluene with no need for external polymer standards and can be used for the determination of the absolute molecular weights of both linear polymer and branched polymers. Laser desorption/ionization-time of flight mass spectrometry (MALDI−TOF MS) spectra were collected on an Applied Biosystems Voyager-DETM STR system. Infrared spectra were recorded on a Perkin-Elmer 100 serial FTIR spectrophotometer calibrated with polystyrene film. Circular dichroism (CD) measurements were carried out on a JASCO J-700 or a JASCO 720 CD spectrometer.

Synthesis of PBLG (Table 1, Entries 1−4). Both linear and block PBLGs were synthesized via the controlled NCA polymerization mediated by N-TMS amines.[29] Hexamethyldisilazane (HMDS) mediated Glu-NCA polymerization yielded linear PBLGs with precisely controlled MW and narrow MWDs (Scheme 1A). The polymerization of Glu-NCA carried out at monomer/initiator (M/I = [Glu-NCA]/[HMDS]) ratios of 28, 41, 78, and 130 resulted in PBLGs with narrowly distributed M_n's of 0.74×10^4 g/mol, 1.09×10^4 g/mol, 2.00×10^4 g/mol and 3.71×10^4 g/mol, respectively, which correspond to DPs of 34, 51, 87, and 169. The M_n, M_w, and MWD (M_w/M_n) were determined by GPC and summarized in Table 1a (entries 1−4). ^{1}H NMR (TFA-d, 500 MHz): δ 7.39−7.25 (ArH−), 5.08 (C$_6$H$_5$CH$_2$−), 4.57 (CH−NH−, αH−), 2.90 (−CH$_2$−, γH−), 2.44, 2.11 (−CH$_2$−, βH−).

Synthesis of PBLG-b-PBLG (Table 1, Entries 5−6). The block copolymer PBLG-b-PBLG were prepared by initiating the Glu-NCA polymerization at both end of the N,N′-bis(trimethylsilyl)cystamine simultaneously (Scheme 1B). We use the term of "block copolymer" here to emphasize the independent folding of two PBLG blocks in the chain. Two polymers at M/I ratios of 50 and 90 were synthesized by following a similar procedure as that for the synthesis of homo-PBLG. The M_n, M_w, and MWD (M_w/M_n) were determined by GPC and summarized in Table 1a (entries 5−6). ^{1}H NMR (TFA-d, 500 MHz): δ 7.39−7.25 (ArH−), 5.08 (C$_6$H$_5$CH$_2$−), 4.57 (CH−NH−, αH−), 2.90 (−CH$_2$−, γH−), 2.44, 2.11 (−CH$_2$−, βH−).

To synthesize N,N′-bis(trimethylsilyl) cystamine, the initiator for the synthesis of PBLG-b-PBLG via NCA polymerization, cystamine dihydrochloride (1.12 g, 5 mmol), dry triethylamine (5 mL) and dry THF (10 mL) were mixed in a nitrogen charged 50 mL round-bottom flask. The mixture was stirred for 8 h. Trimethylsilyl chloride (TMSCl, 1.2 g, 11 mmol) was added to the mixture via a syringe. The mixture was stirred at room temperature for an additional 24 h. The white solid was removed by filtration under nitrogen. After the solvent was removed under vacuum, N, N′-bis(trimethylsilyl) cystamine was obtained as a colorless oil (1.1 g, 74%). ^{1}H NMR (CDCl$_3$, 500 MHz): δ 3.01 (t, 4H, J = 6.5 Hz, NHCH$_2$CH$_2$SSCH$_2$CH$_2$NH), 2.67 (t, 4H, J = 6.5 Hz, NHCH$_2$CH$_2$SSCH$_2$CH$_2$NH), 0.85 (s, broad, 2H,

Table 1. Synthesis of Homo-PBLG and PBLG-Containing Macromolecules with Complex Architecture

entry	polymer	$x(x^*)^a$	$y(y^*)^b$	$n(n^*)^c$	$M_n(M_n^*)^d$ ($\times 10^4$ g/mol)	MWD (M_w/M_n)
1	PBLG$_{34}$	\	\	34(28)	0.74(0.89)	1.23
2	PBLG$_{51}$	\	\	51(41)	1.09(1.35)	1.18
3	PBLG$_{87}$	\	\	87(78)	2.00(2.20)	1.15
4	PBLG$_{169}$	\	\	169(130)	3.71(2.85)	1.07
5	PBLG$_{25}$-b-PBLG$_{25}$	\	\	25(25)	1.08(1.09)	1.23
6	PBLG$_{42}$-b-PBLG$_{42}$	\	\	42(45)	1.83(1.97)	1.28
7	(PN-g-PBLG$_{31}$)$_{18}$	18(20)	0	31(32)	13.8(14.1)	1.03
8	(PN-g-PBLG$_{50}$)$_{17}$	17(20)	0	50(50)	20.1(19.1)	1.13
9	(PN-g-PBLG$_{84}$)$_{18}$	18(20)	0	84(75)	36.2(32.3)	1.05
10	(PN-g-PBLG$_{145}$)$_{18}$	18(20)	0	145(130)	51.7(57.2)	1.3
11	(PN-g-PBLG$_{186}$)$_{18}$	18(20)	0	186(180)	73.5(71.3)	1.38
12	(PN-g-PBLG$_{34}$)$_{23}$-r-PN$_{58}$	23(20)	58(60)	34(30)	20.4(19.1)	1.03
13	(PN-g-PBLG$_{91}$)$_{23}$-r-PN$_{58}$	23(20)	58(60)	91(100)	51.1(48.1)	1.25
14	(PN-g-PBLG$_{76}$)$_8$-r-PN$_{60}$	8(5)	60(55)	76(50)	15.0(10.3)	1.33
15	(PN-g-PBLG$_{97}$)$_8$-r-PN$_{60}$	8(5)	60(55)	97(90)	18.7(17.3)	1.26
16	(PN-g-PBLG$_{119}$)$_8$-r-PN$_{60}$	8(5)	60(55)	119(130)	22.5(24.3)	1.13

^{a} x = the obtained degree of polymerization (DP) of the polymerization with monomer (N-(N'-trimethylsilyl)aminoethylene)-5-norbornene-*endo*-2,3-dicarboximide); x^* = the expected DP of polymerization with monomer M1. ^{b} y = the obtained DP of polymerization with monomer M2 (N-benzyl-5-norbornene-*endo*-2,3-dicarboximide); y^* = the expected DP of polymerization with monomer M2. ^{c} n = the obtained DP of polypeptides; n^* = the expected DP of polypeptides. ^{d} M_n = the obtained M_n; M_n^* = the expected M_n.

N*H*CH$_2$CH$_2$SSCH$_2$CH$_2$N*H*) and 0.05 (s, 18H, (C*H*$_3$)$_3$SiNHCH$_2$CH$_2$SSC-H$_2$CH$_2$NHSi(C*H*$_3$)$_3$). ^{13}C NMR (CDCl$_3$, 500 MHz): δ 43.4, 40.9, and 0.02.

Synthesis of (PN-g-PBLG) and (PN-g-PBLG)-r-PN Brush Polymers (Table 1, Entries 7−16). We synthesized PN-g-PBLG brush polymers and (PN-g-PBLG)-r-PN brush random copolymers according to our reported procedure.[7] Poly(norbornene-*endo*-2,3-dicarboximide) (PN) bearing N-TMS groups was prepared through ROMP in THF or dichloromethane. The grafting densities of the N-TMS group along the PN backbone were tuned by changing the feeding ratio of the norbornene monomers M1 and M2 (Scheme 1, parts C and D). After removal of the solvent under vacuum, the PN polymers were used to initiate the Glu-NCA polymerization *in situ* without further purification. The MW and MWD of all the brush polymers were well controlled as demonstrated by GPC analysis (Figures S1−S3, Supporting Information). The M_n, M_w, and MWD (M_w/M_n) are summarized in Table 1 (entries 7−16). The DP of both backbone PN and grafting PBLG as well as the PBLG grafting density can be predicted and easily controlled using this method. By modulating these three major macromolecular parameters, we synthesized a total of ten different brush-like polymers to investigate the structural variation in their grafted PBLG chains in these macromolecules. ^{1}H NMR (TFA-d, 500 MHz) for PN-g-PBLG (δ 7.39−7.25, 5.08, 4.57, 3.50, 2.90, 2.44, 2.11, 1.92, 1.18), and for (PN-g-PBLG)-r-PN (δ 8.24, 7.39−7.25, 5.59−5.40, 5.08, 4.61, 4.57, 3.50, 2.90, 2.44, 2.11, 1.92, 1.18).

Trifluoroacetic Acid (TFA) Induced Helix-to-Coil Transitions of PBLGs. Solvent induced helix−coil transition studies were carried out on a Bruker DRX 500 MHz spectrometer, using premeasured compositions of TFA-d and CDCl$_3$ as the solvent. PBLG has been extensively studied as a model for the helix-to-coil transition in polypeptides, and the assignments for the proton resonances in both the helix and the coil form have been well established and were followed in this study.[30−32] The effect of TFA-d on the helix-to-coil transition has also been extensively investigated, and it has been determined that homo-PBLG exists as a helix in chloroform solution and is denatured with increasing amounts of TFA. In the studies, at least 2% TFA-d has been added into the solution to prevent the potential aggregation of PBLG chains to form helix bundles. ^{1}H NMR was used to identify different secondary structures of PBLGs based on their different chemical shifts of α-CH. We followed the reported method[33] by using TFA-d to induce the helix−coil transition of PBLG chains for each of 16 polymers we synthesized.

NOESY Study of PBLG-Containing Polymers. Polymers for NOESY experiments were dissolved in 98:2 (v:v) CDCl$_3$-d:TFA-d and sealed in NMR tubes to prevent solvent evaporation. 2D NOESY experiments were performed on a Bruke DRX-500 MHz NMR spectrometer with the $(\pi/2)-t_1-(\pi/2)-\tau_m-(\pi/2)-t_2$ pulse sequence. A total of 2048 K spectra were acquired with t_1 at 0.15 ms. The $\pi/2$ pulse width was 8.4 μs, τ_m was 100 ms, and the delay between acquisitions was 2 s. PBLG$_{51}$, (PN-g-PBLG$_{50}$)$_{17}$, (PN-g-PBLG$_{145}$)$_{18}$, (PN-g-PBLG$_{91}$)$_{23}$-r-PN$_{58}$, (PN-g-PBLG$_{76}$)$_8$-r-PN$_{60}$ and (PN-g-PBLG$_{119}$)$_8$-r-PN$_{60}$ were selected for NOESY studies.

Synthesis of PZLL (Table 2, Entries 1−3). Linear PZLLs were synthesized via the controlled NCA polymerization mediated by N-trimethylsilyl allylamine (Scheme S1A, Supporting Information). In a drybox, ε-Cbz-L-lysine NCA (Lys-NCA) (30 mg, 0.1 mmol) was dissolved in DMF (0.5 mL). The Lys-NCA solution was then added to a DMF solution containing N-trimethylsilyl allylamine (10 μL, 0.1 mmol/mL). The reaction mixture was stirred for 24 h at room temperature. After Lys-NCA was completely consumed (monitored by checking the NCA anhydride band at 1790 cm^{-1} using FT-IR), PZLL was precipitated with methanol and analyzed with GPC. The polymerization of Lys-NCA carried out at M/I ratios of 58, 100, and 150 resulted in PZLLs with narrowly distributed M_n's of 1.09 × 10^4 g/mol, 2.54 × 10^4 g/mol and 3.62 × 10^4 g/mol, respectively, which correspond to DPs of 47, 97, and 138. The M_n, M_w and MWD (M_w/M_n) were determined by GPC and summarized in Table 2 (entries 1−3). ^{1}H NMR (CDCl$_3$, 500 MHz): δ 8.0 (CH−NH−), 7.39−7.25 (Ar*H*−), 5.10 (C$_6$H$_5$-CH$_2$−), 3.95 (C*H*−NH−, α*H*−), 3.10 (NH−CH$_2$−CH$_2$−), 1.90−1.10 (−CH$_2$−, β, γ, δ*H*−).

Synthesis of PN-g-PZLL (Table 2, Entries 4−9). PN-g-PZLL brush polymers were synthesized by following the same procedure as described in the synthesis of PN-g-PBLG (Scheme S1B, Supporting Information). Poly(norbornene-*endo*-2,3-dicarboximide) (PN) bearing N-TMS groups was prepared through ROMP in THF or dichloromethane. After removal of the solvent under vacuum, the PN polymers were used to initiate the Lys-NCA polymerization *in situ* without further purification. The M_n, M_w, and MWD (M_w/M_n) of the six PN-g-PZLL

Scheme 1. Controlled NCA Polymerizations of PBLG-Containing Macromolecules with Different Architectures, Including: (A) Homo PBLG; (B) PBLG Di-Block Copolymers; (C) PBLG Grafted on Homo-Polymer Backbone of Polynorbornene; (D) PBLG Grafted on Random Copolymer Backbone of Polynorbornene
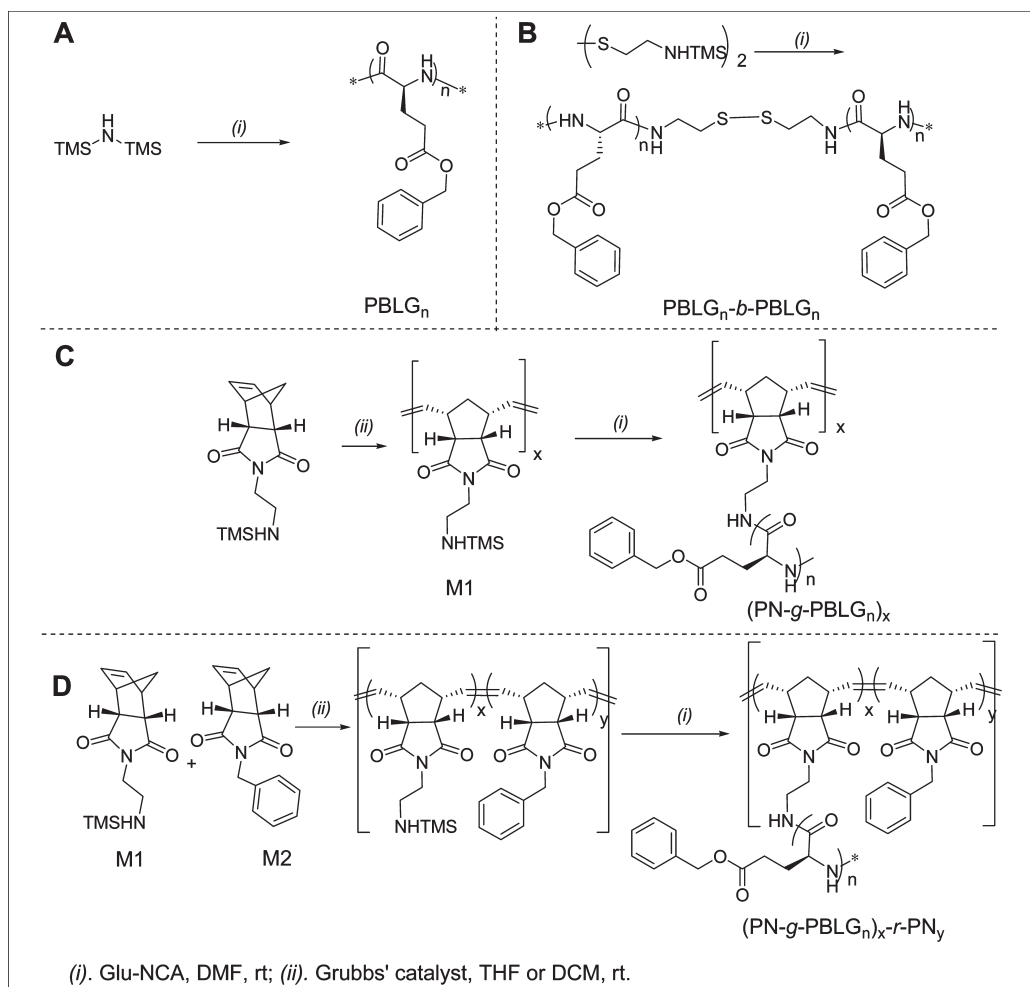

(i). Glu-NCA, DMF, rt; *(ii).* Grubbs' catalyst, THF or DCM, rt.

Table 2. Synthesis of Homo-PZLL and PN-g-PZLL

entry	polymer	$x(x^*)^a$	$n(n^*)^b$	$M_n(M_n^*)^c$ $(\times 10^4 \mathrm{g/mol})$	MWD (M_w/M_n)
1	PZLL$_{47}$	\	47(58)	1.09(1.35)	1.15
2	PZLL$_{97}$	\	97(100)	2.54(2.62)	1.13
3	PZLL$_{138}$	\	138(150)	3.62(3.93)	1.12
4	(PN-g-PZLL$_{50}$)$_9$	9(10)	50 (50)	12.1 (13.3)	1.18
5	(PN-g-PZLL$_{57}$)$_{10}$	10(10)	57(50)	15.1(13.3)	1.05
6	(PN-g-PZLL$_{67}$)$_{10}$	10(10)	67(70)	18.0(18.7)	1.11
7	(PN-g-PZLL$_{70}$)$_9$	9(10)	70(100)	16.6(26.7)	1.27
8	(PN-g-PZLL$_{95}$)$_{10}$	10(10)	95 (100)	25.2(26.7)	1.06
9	(PN-g-PZLL$_{122}$)$_{10}$	10(10)	122(100)	32.2(26.7)	1.38

^{a} x = the obtained degree of polymerization (DP) of the polymerization with monomer (N-(N'-trimethylsilyl)aminoethylene)-5-norbornene-*endo*-2,3-dicarboximide); x^* = the expected DP. ^{b} n = the obtained DP of polypeptides; n^* = the expected DP of polypeptides. ^{c} M_n = the obtained M_n; M_n^* = the expected M_n.

polymers were summarized in Table 2 (entries 4−9). ^{1}H NMR (CDCl$_3$, 500 MHz) for PN-g-PZLL: δ 8.0, 7.39−7.25, 5.10, 3.95, 3.10, 1.90−1.10.

TFA Induced Helix-to-Coil Transitions and NOESY Studies of PZLLs. The structural analysis of PZLLs was carried out by following the same experimental procedures as described for PBLGs.

RESULTS AND DISCUSSION

We applied controlled NCA polymerizations to synthesize a small library of PBLG-containing macromolecules with different architectures, which included (1) homo-PBLG [PBLG$_n$], (2) PBLG block
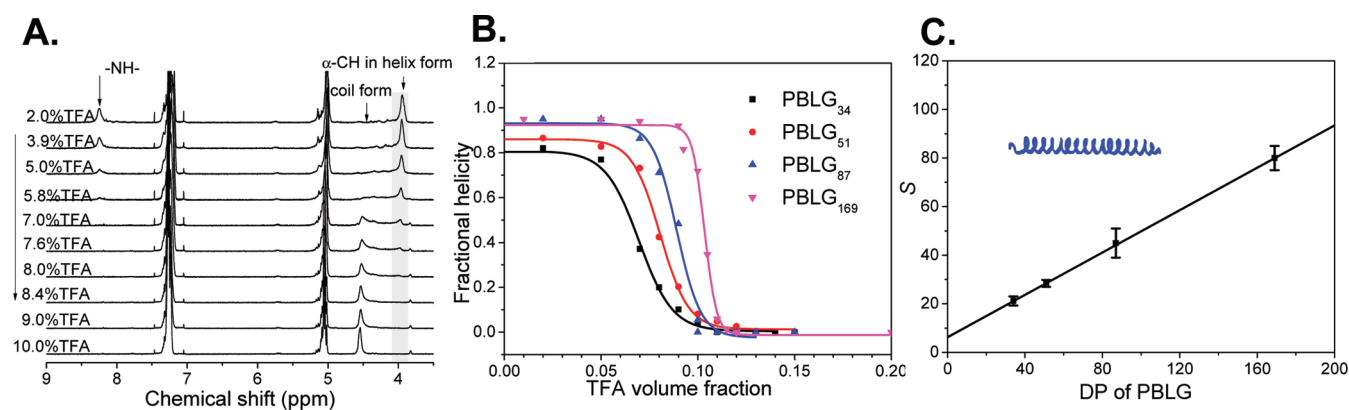
Figure 2. TFA-induced helix-to-coil transition of PBLGs at room temperature. (A) ^{1}H NMR spectra of PBLG$_{34}$ in CDCl$_3$ upon addition of various amount of TFA-*d*. (B) Plot of fractional helicity (determined by ^{1}H NMR) versus volume fraction of TFA-*d* for induced helix-to-coil transition of PBLGs with different chain lengths (DP = 34 (black), 51 (red), 87 (blue), 169 (magenta)). (C) Linear correlation of measured apparent cooperativity (*S*) with DP of homo-PBLG.

copolymer [PBLG$_n$-*b*-PBLG$_n$], (3) PBLG grafted on homo poly-norbornene with ~100% grafting density [(PN-*g*-PBLG$_n$)$_x$], and (4) PBLG randomly grafted on polynorbornene with lower grafting densities [(PN-*g*-PBLG$_n$)$_x$-*r*-PN$_y$] (Scheme 1), where *n*, *x*, and *y* are denoted as the obtained degree of polymerizations (DP) of specific polymer components as described in Table 1. We studied TFA induced helix—coil transitions of PBLGs in these macromolecules to reveal their structural variations in solution.

Prior studies have indicated that the solvent or temperature induced helix—coil transitions of polypeptides are highly cooperative; the "sharpness" of transitions (*S*, or the apparent cooperativity) depends on the helical length of polymers, being sharper at greater chain lengths.[30,31,34−37] In the Schellmann—Zimm—Bragg model,[38−40] the configurations of the polypeptide chains depend upon two parameters: *s*, a helix propagation parameter which is the equilibrium constant for the making of a new helical unit at the end of a helical sequence, and *σ*, a nucleation parameter which is a factor that measures the difficulty of initiating a helical section. Starting with the partition function, the fractional helicity (*θ*, i.e., the fraction of possible hydrogen bonds actually formed in polypeptide chains) was derived as a function of *s*, *σ* and the number of residues (*n*) of polypeptides.[38−40] The midpoint of the helix—coil transition (*θ* = 1/2) occurs when *s* has a critical value of unity[38] (*s*, as an equilibrium constant, can be varied by the change of temperature or solvent). The sharpness of the transition (*S*), which is simply defined as the slope of a *θ* versus *s* plot at midpoint of transition ((d*θ*/d*s*)|$_{s=1}$), shows approximately linear dependence on *n* over a wide range of *n* (see the Supporting Information for the equations).

We attempted to apply this correlation to reveal the structural variations of PBLGs in brush polymers in common helicogenic solvents. To establish a reference system, we first measured the apparent cooperativity of the well-defined, single-helical rods of homo-PBLGs from their solvent induced helix—coil transitions. Homo PBLGs with discrete MWs and narrow MWDs were prepared via HMDS-mediated ring-opening polymerization (ROP) of Glu-NCA (Scheme 1A; entries 1−4, Table 1). Four homo PBLG polymers were synthesized with DPs of 34, 51, 87, and 169. PBLG with DP above 18 is known to form *α*-helix stabilized by intramolecular hydrogen bonds in helicogenic solvents. The homo-PBLGs used in this study, with helical lengths well below the theoretic persistence length of 150 nm,

should adopt a rigid-rod structure in solvents such as chloroform and trifluoroethanol.[39,41−43]

We carried out trifluoroacetic acid (TFA) induced helix—coil transitions of homo PBLGs in chloroform at 25 °C. The PBLG chains change from helices to coils upon the addition of TFA, a strong helix-disrupting solvent.[30] Figure 2A shows the representative spectra of PBLG$_{34}$ at different solvent compositions at 298 K. The chemical shifts of the *α*-proton in *α*-helix and random coil structure of PBLG are 4.0 and 4.6 ppm, respectively. The fraction of *α*-proton existing in the *α*-helix structure was used to calculate the helical contents of PBLGs at a given solvent composition. When the volume fraction of TFA-*d* in the CDCl$_3$/TFA-*d* mixture was gradually increased, the *α*-helix conformation of homo-PBLGs diminished and eventually disappeared, as evidenced by NMR analysis of the chemical shift at around 4.0 ppm.

The complete helix—coil transition process can be presented by plotting the helix contents of PBLGs as a function of volume fraction of TFA-*d* added in the solution. Figure 2B shows the TFA-induced helix—coil transition of the four homo PBLG samples with discrete DPs (Figures S4−S6, Supporting Information). Similar to the classic studies by Zimm,[39] the apparent cooperativity (*S*) of homo-PBLGs, which is defined as the slope at midpoint of transition, increased with PBLG chain length (entries 1−4 in Table 3). The plot of the measured *S* follows a linear correlation with the PBLG chain length in the DP range we studied (Figure 2C), which is expected for helical chains that contain single, continuing helical sequence. In contrast, poly-peptides with the same chain lengths but form "broken" rod-like structures (i.e., two or more helical sequences separated by coil sections), are expected to have significantly reduced *S*. By using the single-helical homo PBLGs as the reference system, we can evaluate the apparent cooperativity (*S*) measured from grafted-PBLGs in brush-like macromolecules, to reveal their structural deviations from ideal single helical rods.

Before we applied this structure-analysis method on grafted-PBLGs in brush polymers, we validated this approach by evaluat-ing the *S* of PBLG chains in block copolymers, a control system with designed "broken rod" structure in which two helical segments of PBLG are separated by a disulfide. Two block copolymers (PBLG$_{25}$-*b*-PBLG$_{25}$ and PBLG$_{42}$-*b*-PBLG$_{42}$) were prepared by initiating the Glu-NCA polymerization at both ends of *N,N'*-bis(trimethylsilyl) cystamine simultaneously (Scheme 1B, Figures

Table 3. Measured Helicity and Apparent Cooperativity of Homo-PBLGs and the PBLG-Containing Macromolecules in Chloroform-*d*

entry	polymer	helicity[a]	apparent cooperativity (S)	$S_{\text{grafted-PBLG}}/S_{\text{PBLG}}$[b]
1	PBLG$_{34}$	0.82	21.2	\
2	PBLG$_{51}$	0.87	28.4	\
3	PBLG$_{87}$	0.95	45	\
4	PBLG$_{169}$	0.95	80	\
5	PBLG$_{25}$-*b*-PBLG$_{25}$	0.76	16.8	\
6	PBLG$_{42}$-*b*-PBLG$_{42}$	0.85	27	\
7	(PN-*g*-PBLG$_{31}$)$_{18}$	0.78	19.6	0.99
8	(PN-*g*-PBLG$_{50}$)$_{17}$	0.81	23.2	0.82
9	(PN-*g*-PBLG$_{84}$)$_{18}$	0.77	26.1	0.6
10	(PN-*g*-PBLG$_{145}$)$_{18}$	0.78	38.2	0.54
11	(PN-*g*-PBLG$_{186}$)$_{18}$	0.76	44.7	0.51
12	(PN-*g*-PBLG$_{34}$)$_{23}$-*r*-PN$_{58}$	0.81	22	1.04
13	(PN-*g*-PBLG$_{91}$)$_{23}$-*r*-PN$_{58}$	0.85	30	0.65
14	(PN-*g*-PBLG$_{76}$)$_{8}$-*r*-PN$_{60}$	0.88	36.4	0.92
15	(PN-*g*-PBLG$_{97}$)$_{8}$-*r*-PN$_{60}$	0.96	42.7	0.88
16	(PN-*g*-PBLG$_{119}$)$_{8}$-*r*-PN$_{60}$	0.9	44.9	0.77

[a] The helicity is measured from the polymers in 2%TFA-d/CDCl$_3$ mixed solutions to avoid potential aggregation of polypeptide chains. [b] In the calculation of $S_{\text{grafted-PBLG}}/S_{\text{PBLG}}$, S_{PBLG} are derived from the calibration curve in Figure 2c.
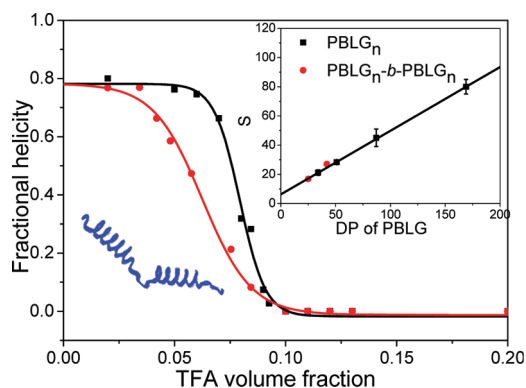

Figure 3. TFA induced helix-to-coil transition for PBLG$_{25}$-*b*-PBLG$_{25}$ (red) and PBLG$_{42}$-*b*-PBLG$_{42}$ (black)). Inset: The apparent cooperativity of PBLG$_n$-*b*-PBLG$_n$ block copolymers depends on the DP (i.e., "*n*") of the individual continuing helical blocks in the macromolecule.

S7–S8, Supporting Information). The overall DP's of these two polymers resemble that of PBLG$_{51}$ and PBLG$_{87}$, respectively. However, the S values of the two polymers determined by the TFA-induced helix–coil transitions (Figure 3 and entries 5–6 in Table 3), are 16.8 and 27.0, respectively, which is much smaller than that of PBLG$_{51}$ and PBLG$_{87}$ (28.4 and 45). Rather, the "S" values of these two PBLG$_n$-*b*-PBLG$_n$ types of copolymers are nearly identical to those of their individual blocks (PBLG$_n$), as their data points perfectly follow the PBLG S ~ DP linear correlation curve when plotted against DP of their individual blocks (inset of Figure 3). These experiments demonstrate that in "broken" rod-like chains, the average helical persistence length (defined here as the average number of residues per continuing helical segments) is strongly correlated with the sharpness of helix–coil transition. Therefore, the measured S can effectively detect the continuousness of helical structure, as "defects" that disrupt the single-helical structures of PBLG will result in reduced helical persistence and a corresponding change in S.

We utilized this structure—analysis approach to elucidate the unknown conformational structures of grafted PBLGs in the brush polymers (PN-*g*-PBLG$_n$)$_x$ and (PN-*g*-PBLG$_n$)$_x$-*r*-PN$_y$. Brush polymers were prepared by integrating ring-opening metathesis polymerization (ROMP) with controlled NCA polymerization, a method that we recently reported (Scheme 1C and 1D). Three groups of brush-like polymers were synthesized to have structures of (PN-*g*-PBLG$_n$)$_{18}$ (*n* = 31, 50, 84, 145, and 186), (PN-*g*-PBLG$_n$)$_{23}$-*r*-PN$_{58}$ (*n* = 34 and 91) and (PN-*g*-PBLG$_n$)$_8$-*r*-PN$_{60}$ (*n* = 76, 97, and 119), which have grafting densities of >99%, 28%, and 12%, respectively (entries 7–16 in Table 1 for MWs and PDI). In these brush polymers, PBLG chains are grafted to a rigid PN backbone and are therefore placed in a locally congested environment. We postulated that, extensive interactions between polypeptide chains with high grafting density would disrupt the single-helical structure of PBLG even in helicogenic solvents and form "broken rod" structures with reduced helical persistence length. Single helices of grafted chains might only exist in the polymers with low grafting densities.

To test this hypothesis, we used the TFA induced helix-to-coil transition study to determine the S of the grafted PBLG chains ($S_{\text{grafted-PBLG}}$) in all synthesized brush-like polymers in chloroform (entries 7–16 in Table 3 and Figures S9–S18, Supporting Information). We found that all of the grafted-PBLGs showed reduced S, as compared to homo-PBLGs with equal chain lengths, suggesting the existence of multiple helical segments in grafted-PBLG chain (Table 3). For quantitative comparison, we normalized the measured $S_{\text{grafted-PBLG}}$ by the corresponding homo-PBLG with equal chain length ($S_{\text{homo-PBLG}}$, determined from the homo PBLG's S~DP linear correlation curve in Figure 2C). The ratio, $S_{\text{grafted-PBLG}}/S_{\text{homo-PBLG}}$, indicates the significance of the structure deviation of the grafted-PBLG from that of corresponding homo-PBLG (i.e., ideal single helices). For instance, a value of 1 indicates a nearly perfect rigid-rod structure, while a value of 0.5 suggests a broken rod structure averaging two helical segments per chain. Figure 4A summarizes
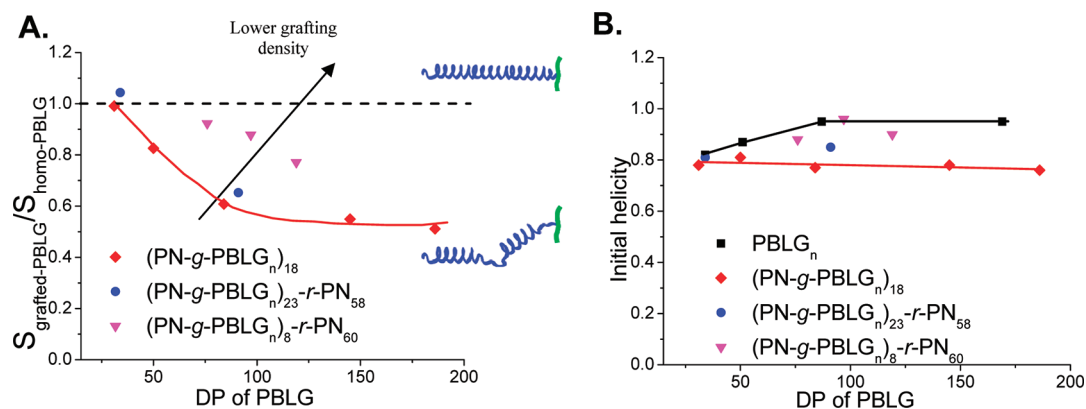
Figure 4. Structural variations of grafted-PBLG chains in brush-like polymers with a rigid PN backbone. (A) Plot of $S_{\text{grafted-PBLG}}/S_{\text{homo-PBLG}}$ as a function of the DP of grafted-PBLG chains [$(\text{PN-}g\text{-PBLG}_n)_{18}$ in red diamond, $(\text{PN-}g\text{-PBLG}_n)_{23}\text{-}r\text{-PN}_{58}$ in blue circles, and $(\text{PN-}g\text{-PBLG}_n)_8\text{-}r\text{-PN}_{60}$ in magenta triangle]. (B) The fractional helicity as a function of the DP of grafted-PBLG chains (PBLG_n in black square, $(\text{PN-}g\text{-PBLG}_n)_{18}$ in red diamond, $(\text{PN-}g\text{-PBLG}_n)_{23}\text{-}r\text{-PN}_{58}$ in blue circles, and $(\text{PN-}g\text{-PBLG}_n)_8\text{-}r\text{-PN}_{60}$ in magenta triangle). The helicity is determined by NMR measurements from the solutions with 2% TFA-d in CDCl_3.

how the normalized apparent cooperativities of grafted PBLGs ($S_{\text{grafted-PBLG}}/S_{\text{homo-PBLG}}$) vary with chain length and grafting density in brush-like polymers. It shows that instead of the formation of presumed single helical chains, multiple helical segments can exist in grafted PBLG, and the "broken" rod structure of grafted-PBLG is strongly dependent on the chain length and the grafting density. At the same grafting density, the elongation of PBLG chains leads to more significant breakdown of the helical structure. For example, for the densely grafted brush polymer with the longest grafted chains $(\text{PN-}g\text{-PBLG}_{186})_{18}$, its $S_{\text{grafted-PBLG}}/S_{\text{homo-PBLG}}$ value was nearly 0.5, indicating that statistically, the 186-mer PBLG grafted chain contains two helical segments. In reality, individual grafted chains may have different numbers and sizes of helical segments. The distribution of different helical segments in the grafted chains can be carefully examined by model-based fitting of the helix—coil transition curve and are the subject of future studies. We also found that, when significantly lowering the grafting density (e.g., to 12%), the conformational structure of PBLG chains (e.g., DP < 100) in brush-like polymers gets close to the ideal rigid rod structure, as evidenced by their corresponding values of $S_{\text{grafted-PBLG}}/S_{\text{homo-PBLG}}$ (Figure 4A and entries 14—16 in Table 3). The fractional helicity of the grafted PBLG measured in the initial helicogenic solvent condition (98:2 CDCl_3:TFA-d) has small but correlated changes with $S_{\text{grafted-PBLG}}/S_{\text{homo-PBLG}}$ (Table 3 and Figure 4B). These results indicate that the smaller values of $S_{\text{grafted-PBLG}}$ compared to $S_{\text{homo-PBLG}}$ are not caused by the formation of long, extended coil sections at chain ends (e.g., induced by the chain tethering on the PN backbone). Instead, the change of helicity measured in the initial helicogenic condition is a consequence of interrupted secondary structures. This also indicates that the multiple helical segments in grafted-PBLG are likely separated by short, extended coil sections.

As the normalized apparent cooperativity ($S_{\text{grafted-PBLG}}/S_{\text{homo-PBLG}}$) can qualitatively describe the extent of disruption of the helical structures, we further looked into whether the interruption of helical chains in brush-like polymers is inherently correlated with the entanglement (or association) behavior of grafted-chains. NOESY experiments were used to reveal the interactions between different grafted-PBLG chains in brush polymers in solution. Figure 5A shows the 2D NOESY spectrum

for $(\text{PN-}g\text{-PBLG}_{50})_{17}$ in 98:2 $\text{CDCl}_3\text{-}d$:TFA-d at 25 °C, obtained with a mixing time of 100 ms. In the NOESY experiments, through-space dipolar interactions lead to the exchanges of magnetization that can be observed as cross (off-diagonal) peaks. Cross peaks connecting several of the resonances were observed for the aromatic and benzylic methylene protons in the grafted PBLG (Figure 5A), showing that these protons are in close contact with α-CH, β-CH, and γ-CH, resulting in an exchange of magnetization (within ~0.5 nm). In the control experiments homo PBLG_{51} (Figure 5B), no cross peaks were observed for the aromatic or benzylic methylene protons in the experimental conditions, resemble to what reported in the previous studies.[44] Therefore, the cross peaks found in the brush-like polymers were resulted from the interactions of grafted PBLG chains, likely due to the slow motions of the aromatic and benzylic methylene protons at the spots of chain entanglement. We subsequently carried out the NOESY studies on four other selected brush polymers (Figures S19—S22, Supporting Information for $(\text{PN-}g\text{-PBLG}_{145})_{18}$, $(\text{PN-}g\text{-PBLG}_{76})_8\text{-}r\text{-PN}_{60}$, $(\text{PN-}g\text{-PBLG}_{119})_8\text{-}r\text{-Pn}_{60}$ and $(\text{PN-}g\text{-PBLG}_{91})_{23}\text{-}r\text{-Pn}_{58}$, respectively), to compare their cross-peak intensities in response to different macromolecular parameters. We found that the normalized intensities of these cross-peaks, which indicate the extent of interactions between grafted chains, are a complex function of both the grafted-chain lengths and the grafting densities in brush polymers (Table S1, Supporting Information). The interactions between grafted PBLGs are more significant with the increase of the chain length and the grafting density. By plotting the normalized intensities of these cross peaks against their normalized apparent cooperativity ($S_{\text{grafted-PBLG}}/S_{\text{homo-PBLG}}$), the data points from five different brush polymers fall onto a master plot which shows a linear correlation between the two parameters (Figure 5C). This strongly indicates an inherent connection between the extents of entanglement among grafted chains and their normalized apparent cooperativity—a measure of structural interruption on the helical chains. In brush polymers, the congested macromolecular environment can cause the entanglement of grafted polypeptides and interrupt the continuousness of their helical structure, even in helicogenic solvents. This leads to the reduced helical persistence of polypeptide chains that can be revealed by measuring the apparent cooperativity of the helical chains, as
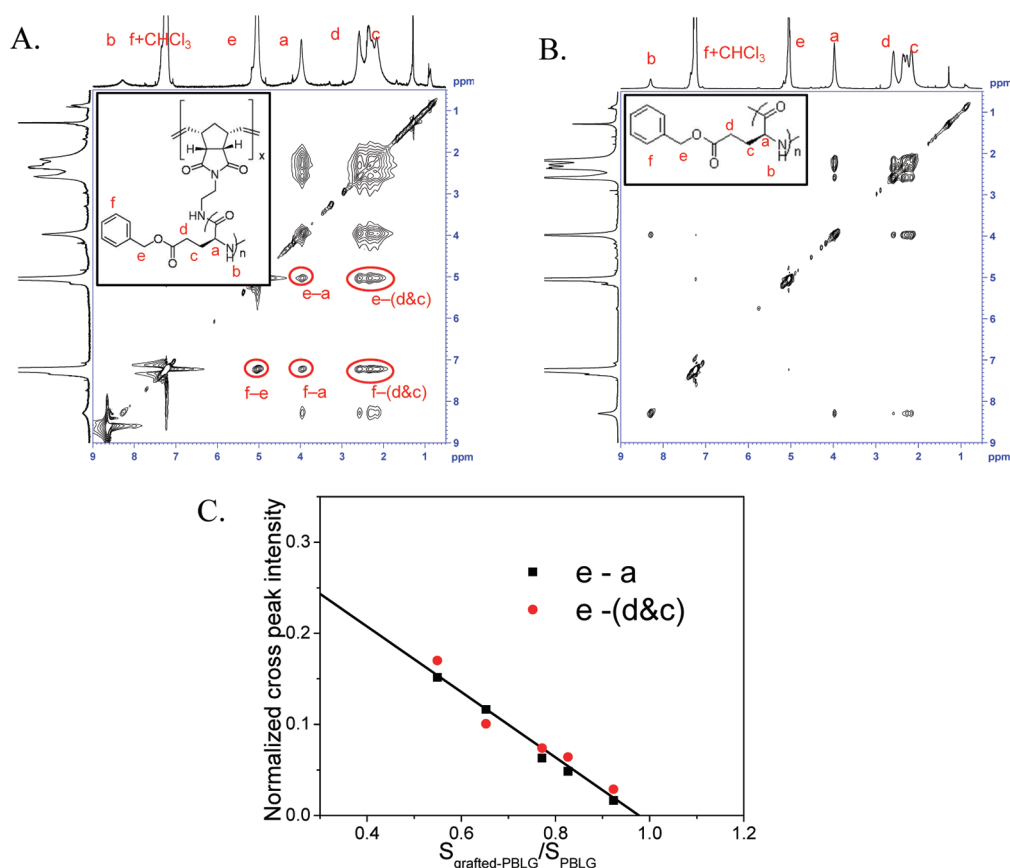
Figure 5. 2D NOESY spectra of (A) $(PN\text{-}g\text{-}PBLG_{50})_{17}$ and (B) $PBLG_{51}$ obtained by the $(\pi/2)\text{-}t_1\text{-}(\pi/2)\text{-}\tau_m\text{-}(\pi/2)\text{-}t_2$ pulse sequence. (C) Correlation between the normalized intensity of selected cross peaks in NOESY and the normalized apparent cooperativity of grafted PBLGs in five different brush polymers $((PN\text{-}g\text{-}PBLG_{50})_{17}, (PN\text{-}g\text{-}PBLG_{145})_{18}, (PN\text{-}g\text{-}PBLG_{76})_8\text{-}r\text{-}PN_{60}, (PN\text{-}g\text{-}PBLG_{119})_8\text{-}r\text{-}PN_{60},$ and $(PN\text{-}g\text{-}PBLG_{91})_{23}\text{-}r\text{-}Pn_{58})$.

Table 4. Measured Helicity and Apparent Cooperativity of Homo-PZLLs and the PN-g-PZLL in Chloroform-d

entry	polymer	helicity[a]	apparent cooperativity (S)	$S_{grafted\text{-}PZLL}/S_{PZLL}$[b]
1	$PZLL_{47}$	0.60	24.8	\
2	$PZLL_{97}$	0.96	81.6	\
3	$PZLL_{138}$	0.96	115.6	\
4	$(PN\text{-}g\text{-}PZLL_{50})_9$	0.86	52.9	1.50
5	$(PN\text{-}g\text{-}PZLL_{57})_{10}$	0.89	57.0	1.36
6	$(PN\text{-}g\text{-}PZLL_{67})_{10}$	0.90	104.1	2.04
7	$(PN\text{-}g\text{-}PZLL_{70})_9$	0.87	104.0	1.94
8	$(PN\text{-}g\text{-}PZLL_{95})_{10}$	0.93	81.8	1.06
9	$(PN\text{-}g\text{-}PZLL_{122})_{10}$	0.89	61.1	0.60

[a] The helicity is measured from the polymers in 2%TFA-d/CDCl$_3$ mixed solutions to avoid potential aggregation of polypeptide chains. [b] In the calculation of $S_{grafted\text{-}PZLL}/S_{PZLL}$, S_{PZLL} are derived from the calibration curve in Figure 6.
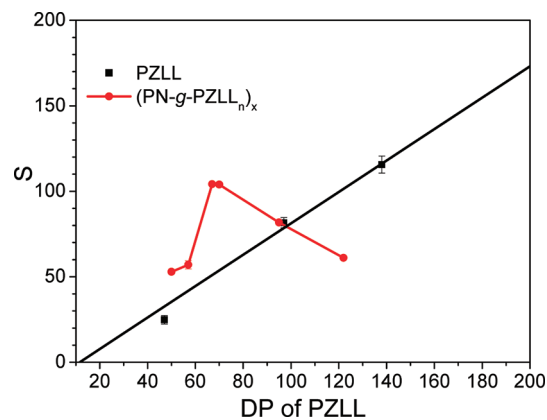

Figure 6. Linear correlation of measured apparent cooperativity (S) of homo-PZLL with DP of homo-PZLL (in black) and the structural variations of grafted-PZLL chains in brush-like polymers with a rigid PN backbone (in red).

each helical segment undergoes independent helix–coil transitions upon the change of environmental conditions.

We expanded our study to include other types of grafted polypeptides. The structure deviations of the grafted-polypeptides from that of corresponding homopolypeptides were also evidenced in other polypeptide-grafted brush polymers. A series of homo-PZLL $[PZLL_n]$ and PZLL grafted on homo polynorbornene

with ~100% grafting density $[(PN\text{-}g\text{-}PZLL_n)_x]$ were synthesized (Table 2, Scheme S1, Supporting Information), and their TFA induced helix–coil transitions were analyzed (Table 4, Figure 6 and Figures S23–S31, Supporting Information). Figure 6 shows that the apparent cooperativity (S) of homo-PZLLs again follows a linear correlation with the PZLL chain length. The normalized apparent cooperativities of grafted-PZLLs $(S_{grafted\text{-}PZLL}/S_{homo\text{-}PZLL})$ in the

brush polymers vary with the chain length (larger than 1 when $n <$ 100, less than 1 when $n > 100$). The result indicates that while short grafted-PZLLs may form bundles which give rise to higher helical cooperativity;[45−47] the formation of multiple helical segments still dominate the folding behavior of the grafted PZLLs with longer chain lengths. NOESY experiments also revealed the extensive interactions between different grafted-PZLL chains in brush polymers in solution (Figures S32−S38, Supporting Information). The additional helical bundling observed in grafted-PZLLs but not in grafted-PBLGs is postulated to arise from the longer side chain of Lys. A systematic study of the side chain effects[48−51] on the folding of polypeptides in a crowded macromolecular environment is the subject of future studies.

CONCLUSION

In conclusion, we successfully applied solvent induced helix−coil transitions to the study of helical structures of polypeptides in brush-like macromolecules. Our study showed that the extensive interchain interactions of densely packed, grafted polypeptides can give rise to an interrupted helical structure. In brush polymers, polypeptides grafted to a rigid backbone are spatially congested in a localized area (i.e., a high "local" concentration) and therefore resemble homo- polypeptides in highly concentrated solutions.[13−15] This "local" concentration of grafted chains is a complex function of grafting density, chain length and backbone rigidity. However, we demonstrated that the normalized apparent cooperativity is a simple and sensitive parameter that can be measured to reveal the subtle structural variations in helical polypeptides. If the conformational structure of grafted polypeptides with large helical persistence is desired in brush-like macromolecules, then the "local concentration" of grafted polypeptides needs to be modulated to avoid unintentional interactions among neighboring polypeptide chains. Our results also showed that the change of the grafting density obtained by incorporating polypeptides on a random copolymer backbone is an effective approach to uninterrupted helical structures of grafted polypeptides, as the grafting density can be varied readily by controlling the compositions in random copolymer. The experimental approach and the structural analysis method described in this report should find applications in the rational design of complex macromolecules with predetermined folding structures as polyvalent scaffolds,[52] platforms for new catalytic systems,[53] and the building blocks for controlled supramolecular assembly.[27]

ASSOCIATED CONTENT

Ⓢ Supporting Information.   Figures showing GPC curves, ^{1}H NMR spectra, and NOESY spectra, a table of normalized intensities of specific cross peaks in NOESY spectra, a scheme showing controlled NCA polymerizations, a Mathematica file, and experimental methods. This material is available free of charge via the Internet at http://pubs.acs.org.

AUTHOR INFORMATION

Corresponding Author
*E-mail: (Y.L.) ylin@ims.uconn.edu; (J.C.) jianjunc@illinois.edu.

ACKNOWLEDGMENT

REFERENCES

(1) Kricheldorf, H. In *Models of Biopolymers by Ring Opening Polymerization*, 1st ed.; Penczek, S., Ed.; CRC Press: Boca Raton, FL, 1989; pp 1−132.

(2) Kricheldorf, H. R. *Angew. Chem., Int. Ed.* **2006**, *45*, 5752–5784.

(3) Hadjichristidis, N.; Iatrou, H.; Pitsikalis, M.; Sakellariou, G. *Chem. Rev.* **2009**, *109*, 5528–5578.

(4) Deming, T. J. *Adv. Mater.* **1997**, *9*, 299–311.

(5) Deming, T. J. *Adv. Polym. Sci.* **2006**, *202*, 1–18.

(6) Choi, T. L.; Grubbs, R. H. *Angew. Chem., Int. Ed.* **2003**, *42*, 1743–1746.

(7) Lu, H.; Wang, J.; Lin, Y.; Cheng, J. J. *J. Am. Chem. Soc.* **2009**, *131*, 13582–13583.

(8) Dimitrov, I.; Schlaad, H. *Chem. Commun.* **2003**, *9*, 2944–2945.

(9) Schlaad, H.; Antonietti, M. *Eur. Phys. J. E* **2003**, *10*, 17–23.

(10) Maynard, H. D.; Okada, S. Y.; Grubbs, R. H. *Macromolecules* **2000**, *33*, 6239–6248.

(11) Roberts, K. S.; Sampson, N. S. *J. Org. Chem.* **2003**, *68*, 2020–2023.

(12) Lu, H.; Cheng, J. J. *J. Am. Chem. Soc.* **2008**, *130*, 12562–12563.

(13) Papadopoulos, P.; Floudas, G.; Klok, H. A.; Schnell, I.; Pakula, T. *Biomacromolecules* **2004**, *5*, 81–91.

(14) Floudas, G.; Spiess, H. W. *Macromol. Rapid Commun.* **2009**, *30*, 278–298.

(15) Papadopoulos, P.; Floudas, G.; Schnell, I.; Lieberwirth, I.; Nguyen, T. Q.; Klok, H. A. *Biomacromolecules* **2006**, *7*, 618–626.

(16) Breitenkamp, R. B.; Ou, Z.; Breitenkamp, K.; Muthukumar, M.; Emrick, T. *Macromolecules* **2007**, *40*, 7617–7624.

(17) Maeda, K.; Kamiya, N.; Yashima, E. *Chem.—Eur. J.* **2004**, *10*, 4000–4010.

(18) Zhang, B.; Fischer, K.; Schmidt, M. *Macromol. Chem. Phys.* **2005**, *206*, 157–162.

(19) Birchall, A. C.; North, M. *Chem. Commun.* **1998**, 1335–1336.

(20) Klok, H. A.; Rodriguez-Hernandez, J. *Macromolecules* **2002**, *35*, 8718–8723.

(21) Irvine, D. J.; Mayes, A. M.; Griffith, L. G. *Biomacromolecules* **2001**, *2*, 85–94.

(22) Biagini, S. C. G.; Parry, A. L. *J. Polym. Sci., Polym. Chem.* **2007**, *45*, 3178–3190.

(23) Klok, H. A.; Langenwalter, J. F.; Locommandoux, S. *Macromolecules* **2000**, *33*, 7819–7826.

(24) Lecommandoux, S.; Achard, M. F.; Langenwalter, J. F.; Klok, H. A. *Macromolecules* **2001**, *34*, 9100–9111.

(25) Cai, C.; Zhu, W.; Chen, T.; Lin, J.; Tian, X. *J. Polym. Sci., Part A: Polym. Chem.* **2009**, *47*, 5967–5978.

(26) Mondeshki, M.; Mihov, G.; Graf, R.; Spiess, H. W.; Mullen, K.; Papadopoulos, P.; Gitsas, A.; Floudas, G. *Macromolecules* **2006**, *39*, 9605–9613.

(27) Wang, J.; Lu, H.; Kamat, R.; Pingali, S. V.; Urban, V. S.; Cheng, J. J.; Lin, Y. *J. Am. Chem. Soc.* **2011**, *133*, 12906–12909.

(28) Love, J. A.; Morgan, J. P.; Trnka, T. M.; Grubbs, R. H. *Angew. Chem., Int. Ed.* **2002**, *41*, 4035–4037.

(29) Lu, H.; Cheng, J. J. *J. Am. Chem. Soc.* **2007**, *129*, 14114–14115.

(30) Bradbury, E. M.; Carpenter, B. G.; Grane-Robinson, C.; Rattle, H. W. E. *Nature* **1968**, *220*, 69–72.

(31) Bradbury, E. M.; Crane-Robinson, C.; Goldman, H.; Rattle, H. W. E. *Nature* **1968**, *217*, 812–816.

(32) Markley, J. L.; Meadows, D. H.; Jardetzky, O. *J. Mol. Biol.* **1967**, *27*, 25–40.

(33) Goodman, M.; Masuda, M. *Biopolymers* **1964**, *2*, 107–112.

(34) Bradbury, E. M.; Fenn, M. D. *Aust. J. Chem.* **1969**, *22*, 357–371.

(35) Doty, P.; Bradbury, J. H.; Holtzer, A. M. *J. Am. Chem. Soc.* **1956,** *78,* 947–954.

(36) Doty, P.; Yang, J. T. *J. Am. Chem. Soc.* **1956,** *78,* 498–500.

(37) Dill, K. A. *Protein Sci.* **1999,** *8,* 1166–1180.

(38) Zimm, B. H.; Bragg, J. K. *J. Chem. Phys.* **1959,** *31,* 526–535.

(39) Zimm, B. H.; Doty, P.; Iso, K. *Proc. Natl. Acad. Sci. U.S.A.* **1959,** *45,* 1601–1607.

(40) Schellman, J. A. *J. Phys. Chem.* **1958,** *62,* 1485–1494.

(41) Schmidt, M. *Macromolecules* **1984,** *17,* 553–560.

(42) Miller, W. G.; Flory, P. J. *J. Mol. Biol.* **1966,** *15,* 298–314.

(43) Helfrich, J.; Hentschke, K.; Apel, U. M. *Macromolecules* **1994,** *27,* 472–482.

(44) Mirau, P. A.; Bovey, F. A. *J. Am. Chem. Soc.* **1986,** *108,* 5130–5134.

(45) Betz, S. F.; Bryson, J. W.; DeGrado, W. F. *Curr. Opin. Struct. Biol.* **1995,** *5,* 457–463.

(46) Ghosh, K.; Dill, K. A. *J. Am. Chem. Soc.* **2009,** *131,* 2306–2312.

(47) DeGrado, W. F.; Gratkowski, H.; Lear, J. D. *Protein Sci.* **2003,** *12,* 647–665.

(48) Lu, H.; Wang, J.; Bai, Y.; Lang, J. W.; Liu, S.; Lin, Y.; Cheng, J. *Nat. Comm.* **2011,** *2:206* DOI: 10.1038/ncomms1209.

(49) Lyu, P. C.; Sherman, J. C.; Chen, A.; Kallenbach, N. R. *Proc. Natl. Acad. Sci. U.S.A.* **1991,** *88,* 5317–5320.

(50) Doig, A. J.; Sternberg, M. J. E. *Protein Sci.* **1995,** *4,* 2247–2251.

(51) Chakrabarti, P.; Pal, D. *Prog. Biophys. Mol. Biol.* **2001,** *76,* 1–102.

(52) Mammen, M.; Choi, S. K.; Whitesides, G. M. *Angew. Chem., Int. Ed.* **1998,** *37,* 2755–2794.

(53) Terashima, T.; Mes, T.; De Greef, T. F. A.; Gillissen, M. A. J.; Besenius, P.; Palmans, A. R. A.; Meijer, E. W. *J. Am. Chem. Soc.* **2011,** *133,* 4742–4745.